FROM POINT TO SLOPE: ASSESSING WEATHER STATION SNOW DEPTH REPRESENTATIVENESS USING LIDAR AND GEOSTATISTICS

Katreen M. Wikstrom Jones[1]*, Gabriel J. Wolken[1,2], and Michael Janes[3]

1 Alaska Division of Geological & Geophysical Surveys, Anchorage/Fairbanks, Anchorage, AK, USA
2 Alaska Climate Adaptation Science Center, University of Alaska, Fairbanks, AK, USA
3 Alaska Electric Light & Power, Juneau, AK, USA

ABSTRACT: Weather station data are widely used by avalanche forecasters to validate meteorological forecasts and to assess snowpack characteristics at specific sites. However, when stations are located in terrain that is not representative, due to slope, aspect, or exposure, this extrapolation can introduce systematic over- or underestimation of snow depth at the slope scale. Such representativeness errors propagate uncertainty into avalanche hazard assessments that typically rely on sparse point observations. Alaska Electric Light and Power (AEL&P) operates a hydroelectric transmission line between Snettisham Hydroelectric Facility and Juneau in southeast Alaska, crossing multiple avalanche paths. Along Speel Arm, the line traverses steep fjord walls and avalanche exposure is particularly high. Following a destructive avalanche in 2008, AEL&P implemented an avalanche mitigation program that included the installation of weather stations to monitor snowpack conditions. One weather station is located on a mid-slope bench (“the Balcony”) and the other is at an avalanche diverter structure further downslope (“Diverter 4-4”). Data from these stations are used to assess snowpack stability in nearby avalanche starting zones. In this study, we evaluate the spatial representativeness of weather stations using spatially distributed snow depth information. We conducted seven airborne lidar surveys in 2019-2023 and produced high-resolution snow depth datasets of the Speel Arm study area. Using geostatistical methods, we characterize spatial snow depth patterns, quantify elevational gradients, and generate difference maps to examine interannual and seasonal variability. We then compare station observations with lidar-derived snow depths using buffer-based sampling and correlation analysis to evaluate their ability to represent slopes-scale conditions and as predictors for absolute and evolutionary snow depth in nearby avalanche starting zones. Results show consistent interannual patterns in snow depth across elevations and persistent late-season snow retention throughout the study area. Our station-focused analysis shows high spatial snow depth variability at the weather station sites. Our distance-weighted correlation model shows that weather station snow depth is not a reliable proxy for snow conditions in selected avalanche starting zones at Speel Arm. Our project findings highlight the limitations of extrapolating point measurements to slope-scale problems while providing guidance for improved weather station placement.

KEYWORDS: Weather stations, Snow Depth, Spatial Representativeness, Snow Prediction, Lidar.

1. INTRODUCTION

Snow depth in mountain catchments is highly heterogenous, with important implications for water storage, alpine ecosystem processes, and natural hazards (Grunewald and Lehning, 2011). Spatial patterns of snow accumulation are controlled by precipitation–elevation relationships, which influence precipitation phase and snowfall distribution, and are subsequently modified by wind redistribution and avalanche activity, producing pronounced variability over short distances (Grunewald and Lehning, 2011).

* Corresponding author address:
Katreen Wikstrom Jones, Alaska Division of Geological & Geophysical Surveys,
Anchorage, AK, 99508, United States
tel: +1 907-268-8051;
email: katreen.wikstromjones@alaska.gov

Fixed weather stations rarely represent snow conditions in avalanche starting zones, where precipitation type, wind transport, and microclimatic variability interact across complex terrain. Stations are typically installed in sheltered locations to improve accessibility, reduce wind-related measurement errors, and facilitate long-term maintenance. Despite these limitations, weather station observations remain a fundamental component of operational avalanche forecasting, particularly in remote, data-sparse regions such as Speel Arm, southeast Alaska, where they may provide the only continuous snowpack information available between storms. Evaluating how well these stations represent surrounding avalanche terrain is therefore essential for understanding the confidence that can be placed in operational forecasting decisions.

Remotely sensed, spatially distributed snow depth mapping can provide valuable information



Figure 1: Speel Arm study area including location of transmission line, towers, diverters and weather stations. (Photo: Wikstrom Jones)

for optimizing weather station placement and evaluating station representativeness (e.g., Herbert et al., 2024; Peitzsch et al., 2018). Previous studies have shown that snow depth exhibits strong, but spatially variable, elevation gradients (Grunewald and Lehning, 2011), while comparisons of weather station observations with lidar-derived snow depth have demonstrated that stations are often biased toward deeper snow because they are preferentially located in sheltered terrain (Herbert et al., 2024). These findings highlight the need to assess whether existing station locations adequately characterize surrounding avalanche terrain.

In this study, we use airborne lidar to map snow depth across the Speel Arm study area and evaluate the spatial representativeness of two automated weather stations. We (1) quantify elevational snow depth gradients and patterns of late-season snow retention, (2) compare station snow depth with lidar-derived snow depth within a local buffer surrounding each station, and (3) assess the similarity between snow conditions at the stations and nearby avalanche starting zones to identify locations that better represent terrain-scale snow distribution.

2. STUDY AREA

The study area is located in the Speel Arm fjord south of Juneau, southeast Alaska. The avalanche terrain consists of a large bowl, cliff bands, a mid-slope bench ("the Balcony"), and steep forested gullies that form several distinct avalanche paths (Figure 1). The AEL&P power transmission line traverses the lower slope, crossing avalanche paths either within their runout zones or farther upslope before descending toward the Snettisham Hydroelectric Facility.

Speel Arm has a maritime snow climate characterized by heavy, wet winter storms and a fluctuating rain–snow line. Most precipitation is associated with southerly to southwesterly storms, while strong northerly outflow winds frequently redistribute snow across the slope (Figure 2).

Following a destructive avalanche in 2008, AEL&P implemented a comprehensive avalanche mitigation program that included automated weather stations for snowpack monitoring. This study evaluates two stations: the Balcony station (569 m asl), located on the mid-slope bench, and the Diverter 4-4 station (229 m asl),

situated on an avalanche diverter structure (Figure 1). Both stations continuously measure air temperature, relative humidity, wind speed and direction, and snow depth using ultrasonic sensors.

3. METHODOLOGY

3.1 Snow depth mapping using aerial lidar

Airborne lidar surveys were conducted to map bare-ground ("snow-off") and snow-covered ("snow-on") surface elevations at Speel Arm. Using a fixed-wing aircraft–mounted lidar system, we acquired a 50 cm snow-off dataset on 2019-09-07, followed by 1 m snow-on datasets on 2020-02-02, 2020-03-13, 2021-03-04, 2021-04-16, 2022-04-21, and 2023-04-19. Survey details and product accuracy are reported in Wikstrom Jones et al. (2022).

Snow-on digital terrain models (DTMs) were coregistered to the bare-ground DTM by correcting horizontal offsets at the 4-4 Diverter and vertical offsets using shoreline bedrock outcrops. Snow depth rasters were generated by subtracting bare-ground elevations from each snow-on DTM.

Geostatistical analysis

We conducted a set of geostatistical analyses to better understand snow distribution patterns and relationships at Speel Arm. First, we quantified mean elevational snow depth gradients for each lidar acquisition date by averaging snow depths within 10 m elevation bins. Next, we analyzed late-season snow retention patterns using the April lidar surveys from 2021–2023. To compare relative snow distribution between years, each snow depth raster was normalized using Z-scores:

$$Z = \frac{X - \mu}{\sigma} \qquad (1)$$

where X is pixel snow depth value, μ is full area mean snow depth, and σ is standard deviation. The normalized snow depth rasters were combined into a composite multiband raster and classified into five groups using the *Iso Cluster Unsupervised Classification* workflow in ArcGIS Pro (ESRI, 2026). This tool first applies an isodata clustering algorithm to group raster cells with similar multidimensional attributes into statistically distinct clusters. Then it applies Maximum Likelihood Classification which uses statistical characteristics derived from the cluster signatures to classify raster cells, assuming a normal (Gaussian) distribution in multidimensional feature space, and then employs Bayesian probability to assign each cell to the most likely class. Because the input rasters were normalized, the resulting clusters represent relative snow retention patterns rather than absolute snow depth.

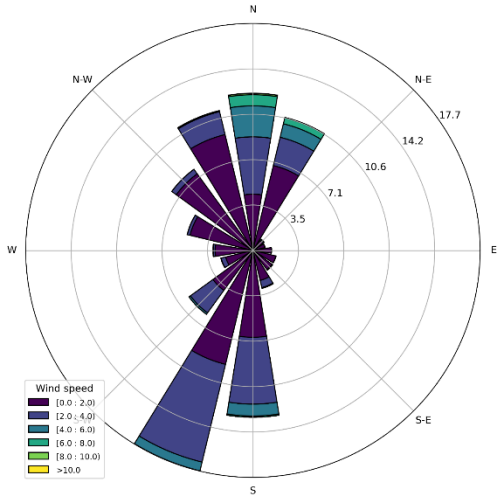


Figure 2: Frequency percentage of wind direction and speed recorded at Balcony weather station from 2014-03-23 to 2025-09-14.

Weather station representativeness was evaluated by calculating mean snow depth and snow depth range within progressively larger buffers surrounding each station (Herbert et al., 2024). Lidar-derived snow depth within a 1 m buffer was also compared with station observations to assess local measurement agreement.

To evaluate how well station observations predicted snow conditions in nearby avalanche starting zones, measured snow depth at the Balcony and Diverter 4-4 stations were used to estimate mean snow depth in the avalanche starting zones using inverse distance weighting (IDW):

$$HS_Pred_{Zone}(t) = w_1 \cdot HS_{Div}(t) + w_2 \cdot HS_{Balc}(t) \qquad (2)$$

where *HS* stands for "height of snowpack" (more commonly referred to as snow depth), w_1 and w_2 are distance-weights. Distances, *d*, between each avalanche starting zone centroid and weather station were converted to weights according to:

$$w_i = \frac{1/d_i^2}{\sum_j 1/d_j^2} \qquad (3)$$

A second analysis used only the Diverter 4-4 station to predict snow depth in the adjacent 4-3 and 4-4 starting zones. Model performance was evaluated using Pearson's correlation coefficient, p-value, coefficient of determination (R^2), root-mean-square-error (RMSE), bias (predicted value – observed value) and mean absolute error (MAE).

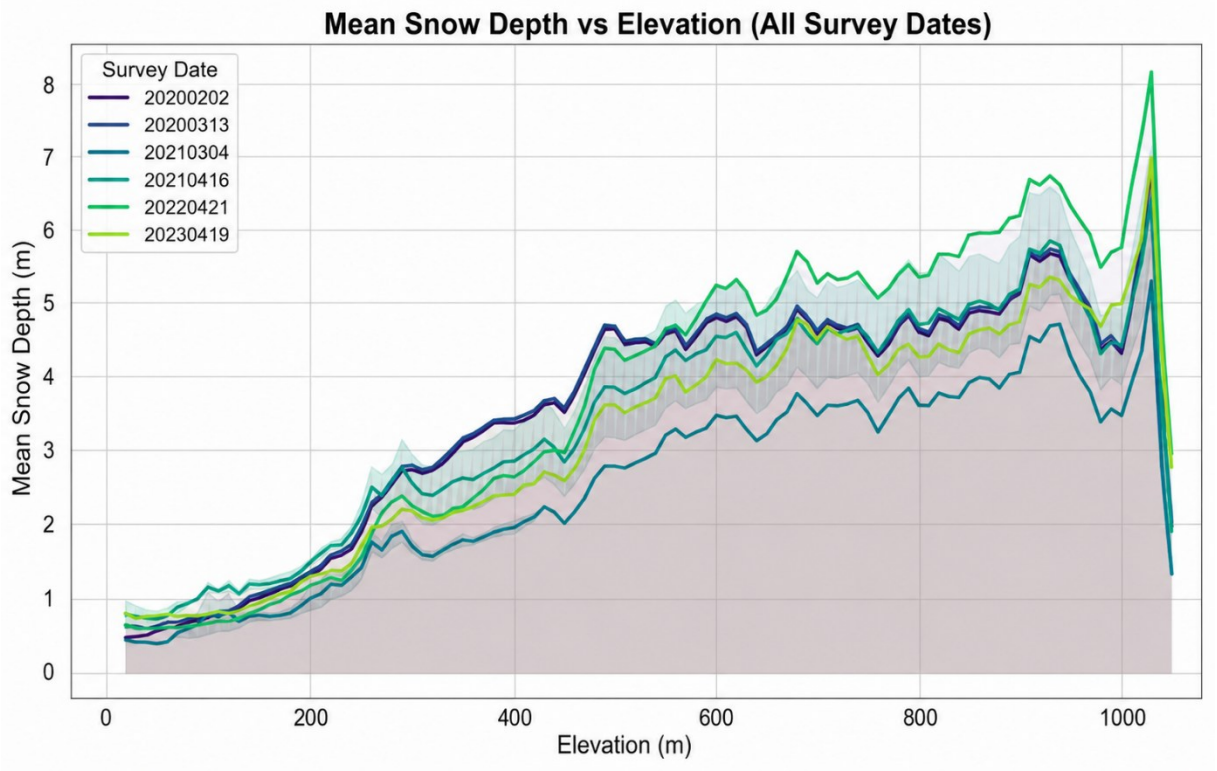


Figure 3: Elevational snow depth gradient for Speel Arm using all lidar acquisitions and averaged for 10 m elevation bins.

Finally, we used zonal statistics to calculate intraseasonal mean snow depth change within each starting zone for two periods in 2020 and 2021. A two-year raster similarity analysis was then performed using Euclidean distance *D*:

$$D = \sqrt{(r_{2020} - \mu_{2020})^2 + (r_{2021} - \mu_{2021})^2} \quad (4)$$

where *r* is the pixel-scale snow depth change and *μ* the mean snow depth change within each avalanche starting zone. Pixels with low Euclidean distance exhibited snow accumulation and ablation patterns most similar to those observed in the reference avalanche starting zone.

4. RESULTS & DISCUSSION

4.1 Elevational snow depth gradient

Across the survey dates, mean snow depth increased with elevation to approximately 600 m asl, consistent with enhanced orographic precipitation and cooler temperatures. Above ~600 m asl, the gradient weakened and snow depth variability increased (Figure 3), indicating that wind redistribution and local topographic controls became more important than elevation alone. Maximum snow depths consistently occurred between 900 and 1000 m asl (Figure 3) where drifting and terrain-driven deposition likely promote preferential accumulation.

4.2 Interannual snow retention patterns

Late-season snow retention patterns were highly consistent among the 2021–2023 surveys (Figure 4). The five cluster classes represent persistent relative snow retention, ranging from consistently snow-poor (Class 1) to extreme snow retention (Class 5) (Table 1). Low-retention classes occurred primarily on exposed ridges, convex slopes, and south-facing terrain, whereas persis-

Table 1: Cluster class descriptions.

Class	*2021 Mean Hs*	*2022 Mean Hs*	*2023 Mean Hs*	*Relative to average Hs*	*Interpretation—Snow retention*
1	-0.87	-0.86	-0.92	Strongly below average	**Persistently low**
2	-0.24	-0.25	-0.30	Slightly below average	**Slightly low**
3	+0.43	+0.45	+0.39	Slightly above average	**Moderate**
4	+1.26	+1.28	+1.24	Clearly above average	**Persistently high**
5	+2.62	+2.63	+2.59	Outlier-level anomaly	**Extreme**

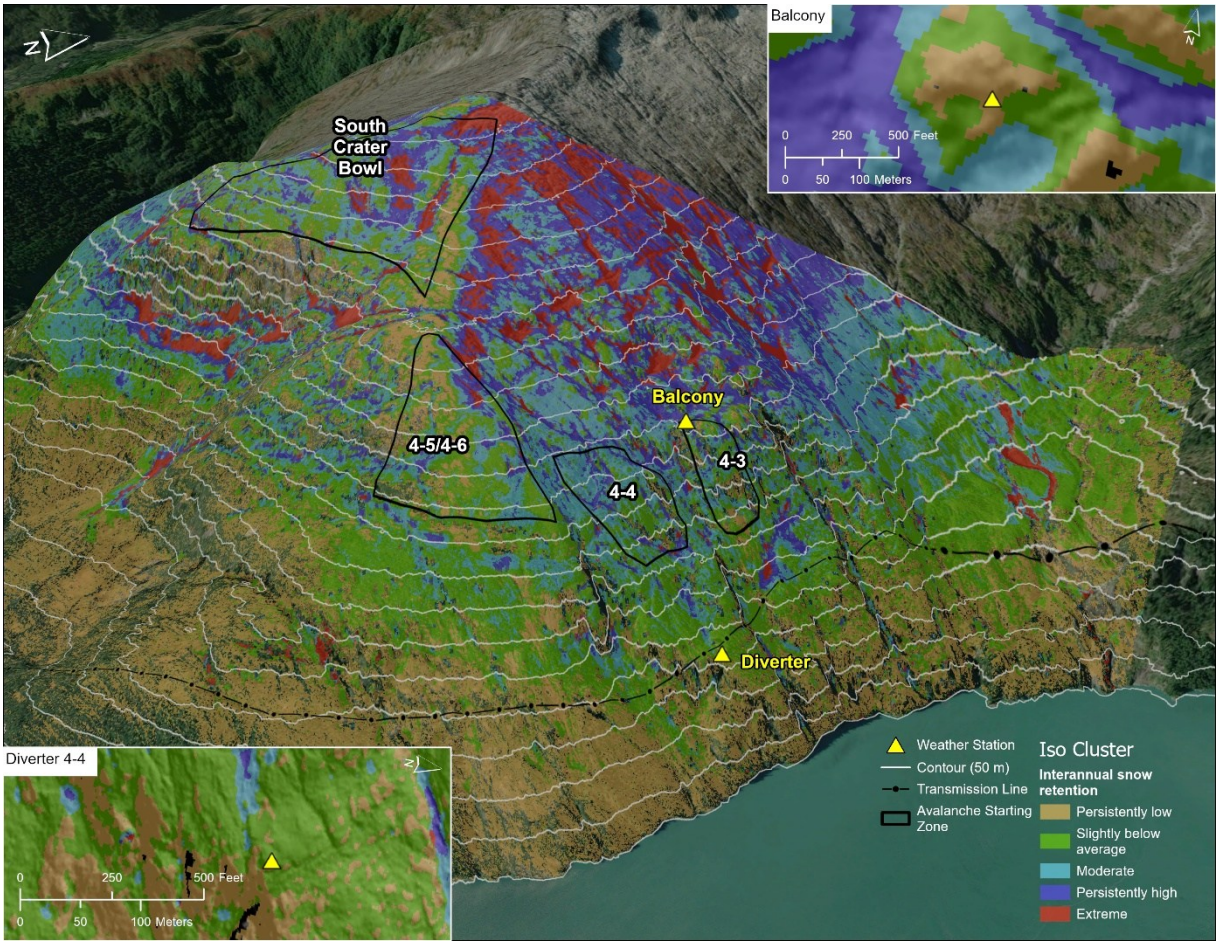


Figure 4: Late-season snow retention patterns based on Unsupervised Iso Cluster Classification analysis, using Z-score normalized 2021-04-16, 2022-04-21 and 2023-04-19 lidar-derived snow depth raster.

tent accumulation was associated with sheltered bowls, gullies, avalanche deposition zones, and other terrain traps (Figure 4).

Snow retention appears to be strongly controlled by aspect, reflecting preferable lee-side slopes for wind-redistributed snow. Zones of extreme snow retention below the cliffs of South Crater Bowl starting zone are snow shedding/avalanche deposition areas. Surrounding the Balcony weather station, we find both persistently low and persistently high snow retention areas, with the station itself located in what appears to be a persistently low-below average zone (Figure 4).

4.3 *Spatial scaling of snow depth around weather stations*

Mean snow depth around the Balcony station increased with buffer radius, indicating that the station is located in a relatively snow-poor area compared to the surrounding terrain (Figure 5). This suggests that local topography influences snow accumulation and that measurements at the station may not fully represent nearby snow conditions. In contrast, mean snow depth around the Diverter 4-4 station changed little beyond a 10 m buffer, indicating relatively uniform snow conditions in its immediate surroundings. As expected, snow depth variability (range) increased with buffer radius at both stations as larger areas encompassed more diverse terrain (Figure 5). Within the 50 m buffers, snow depths ranged from shallow, wind-scoured surfaces to drifts approaching 20 m in sheltered gullies and other preferential deposition zones.

4.4 *Station-measured vs. lidar-derived snow depth*

Lidar-derived and station-measured snow depths generally agreed, although differences exceeded 2 m on several survey dates, particularly near peak accumulation (RMSE = 0.98 m). These discrepancies likely reflect strong microtopographic variability surrounding the station, together with limitations inherent to ultrasonic snow-depth measurements over irregular snow surfaces (McClung and Schaerer, 2006; Campbell Scientific, 2026). Sonic ranging sensors measure snow depth by timing the return of an acoustic pulse

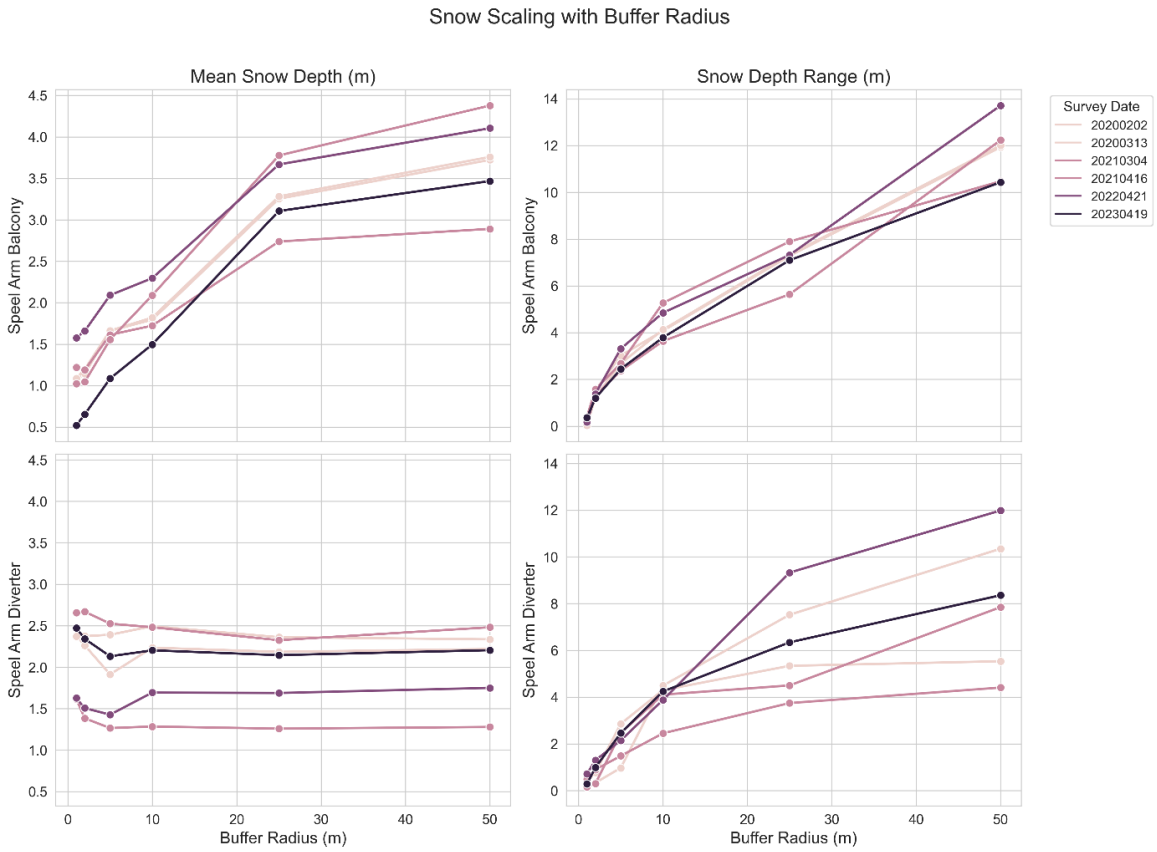


Figure 5: Mean snow depth and mean snow depth range per buffer size at the Balcony and Diverter 4-4 weather stations. Snow depth values derived from lidar acquisitions labeled by survey date.

reflected from the snow surface. The measurement represents an average over the sensor footprint, which decreases as the snowpack deepens. Rough or irregular snow surfaces can produce noisy or inconsistent returns (Campbell Scientific, 2026). In addition, ultrasonic sensors have a minimum operating distance, making adequate installation height essential for measuring maximum snow depths. The Diverter 4-4 sensor is mounted 3 m above the ground.

4.5 Predictive skill

The distance-weighted model showed poor predictive skill for estimating mean snow depth in avalanche starting zones from weather station observations (Pearson r: 0.166, p-value: 6.062e-01, R^2: -8.403, RMSE: 2.556 m, Bias (Pred - Obs): -2.242 m, MAE: 2.298 m). While some temporal variability is captured, the model fails to represent key physical controls, including elevational gradient, wind redistribution and microclimatic effects. This is likely compounded by station placement in lower-elevation terrain relative to the preferentially wind-loaded, complex terrain of avalanche starting zones. In addition, missing Balcony station observations for 2020-2021 further reduce model completeness during key lidar acquisition periods. A simplified model using only the Diverter 4-4 station produced more consistent error metrics but remained a poor predictor of starting-zone snow depth (Figure 6).

The Diverter 4-4 station also failed to capture intraseasonal snow depth changes within the adjacent 4-3 and 4-4 avalanche starting zones. During both study periods (2 February–13 March 2020 and 4 March–16 April 2021), the station recorded snowpack losses (2020: −1.05 m; 2021: −0.91 m), whereas the avalanche starting zones experienced stable or increasing snow depths (2020: +0.02 m and +0.03 m; 2021: +1.41 m and +1.95 m, respectively). This divergence indicates that the starting zones can continue to accumulate or retain snow while lower-elevation stations experience snow depletion, likely reflecting differences in precipitation phase due to elevation and wind redistribution.

These findings highlight the limitations of using point-based snow depth measurements to represent spatially integrated snow conditions in complex avalanche terrain. Improving predictive skill will likely require relocating weather stations to higher elevations where snowpack evolution more closely resembles that of avalanche starting zones.

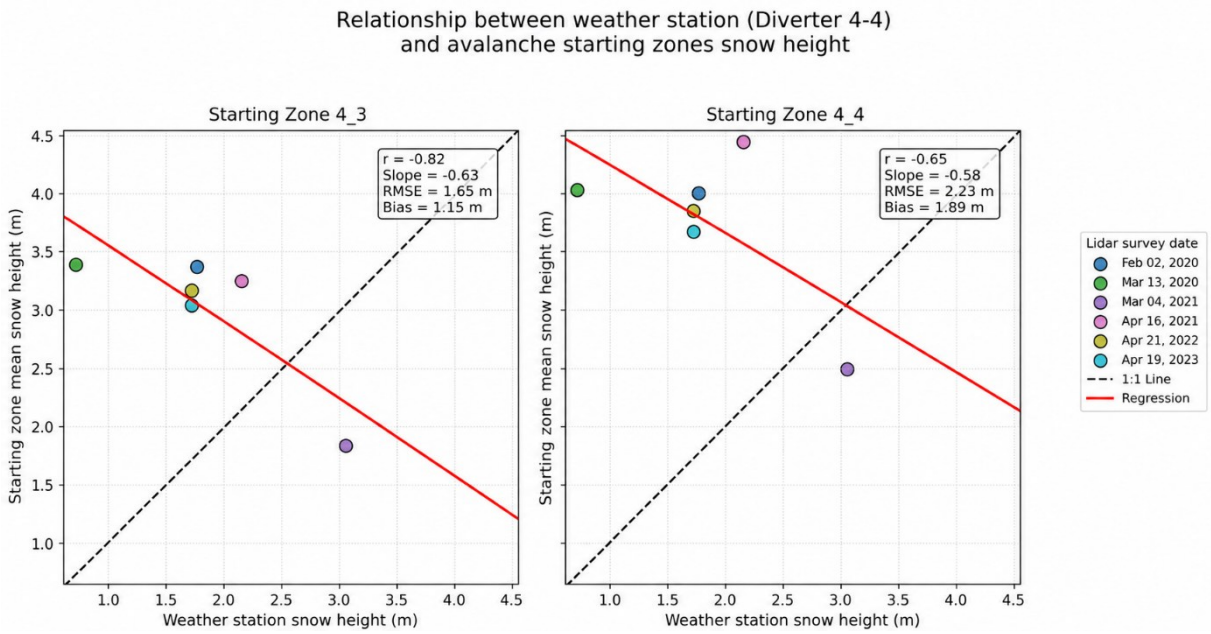


Figure 6: Regression and correlation analysis of snow depth predicted by the Diverter 4-4 station and mean snow depth in the 4-3 and 4-4 avalanche starting zones on lidar survey dates.

4.6 Similarity analysis for weather station placement

The similarity analysis identified areas across the study area with snow accumulation and ablation patterns comparable to those of the four avalanche starting zones (Figure 7). Most pixels most closely resembled the South Crater Bowl and 4-4 starting zones, whereas substantially fewer areas exhibited snow depth change patterns similar to the 4-3 and combined 4-5/4-6 starting zones. Several candidate locations representing all four starting zones occur near the existing Balcony weather station, suggesting that relatively minor relocations could improve the representativeness of weather station observations while maintaining accessibility. Final site selection should also consider slope angle and avalanche hazard to ensure placement outside avalanche release and runout zones.

5. CONCLUSION

This study combined airborne lidar data with geostatistical analyses to characterize spatial patterns of snow distribution in Speel Arm and evaluate how well AEL&P's weather stations represent avalanche starting zones. High resolution lidar-derived snow depth maps revealed consistent spatial patterns of snow accumulation and retention across multiple winters, with snow depth increasing up to ~600 m of elevation, above which terrain-driven processes such as wind redistribution and avalanche deposition exert stronger controls. Analyses of station representativeness showed that the existing stations do not adequately capture snowpack variability in nearby avalanche starting zones, resulting in limited predictive skill for estimating both snow depth and seasonal change. In particular, the Diverter 4-4 station fails to represent accumulation trends at higher-elevation starting zones during key periods of the winter season. Building on these findings, AEL&P plans to use the map products developed in this study to identify suitable locations for additional snow depth sensors closer to the avalanche starting zones while remaining outside avalanche-prone terrain. While our analysis is constrained by a relatively short lidar record, variable acquisition timing, and incomplete station data, the consistency of observed spatial patterns and station representation across years supports the robustness of these findings. By identifying locations with snow dynamics more closely aligned with starting zones, this work demonstrates that relatively minor adjustments in station siting can substantially improve the relevance of in situ observations and provides a transferable framework for evaluating and optimizing weather station placement in complex terrain.

ACKNOWLEDGEMENTS

This work was funded by U.S. Geological Survey Climate Adaptation Science Center, Alaska Electric Light & Power, and the State of Alaska. We thank Coastal Helicopters for their aviation expertise and contribution to these data products.

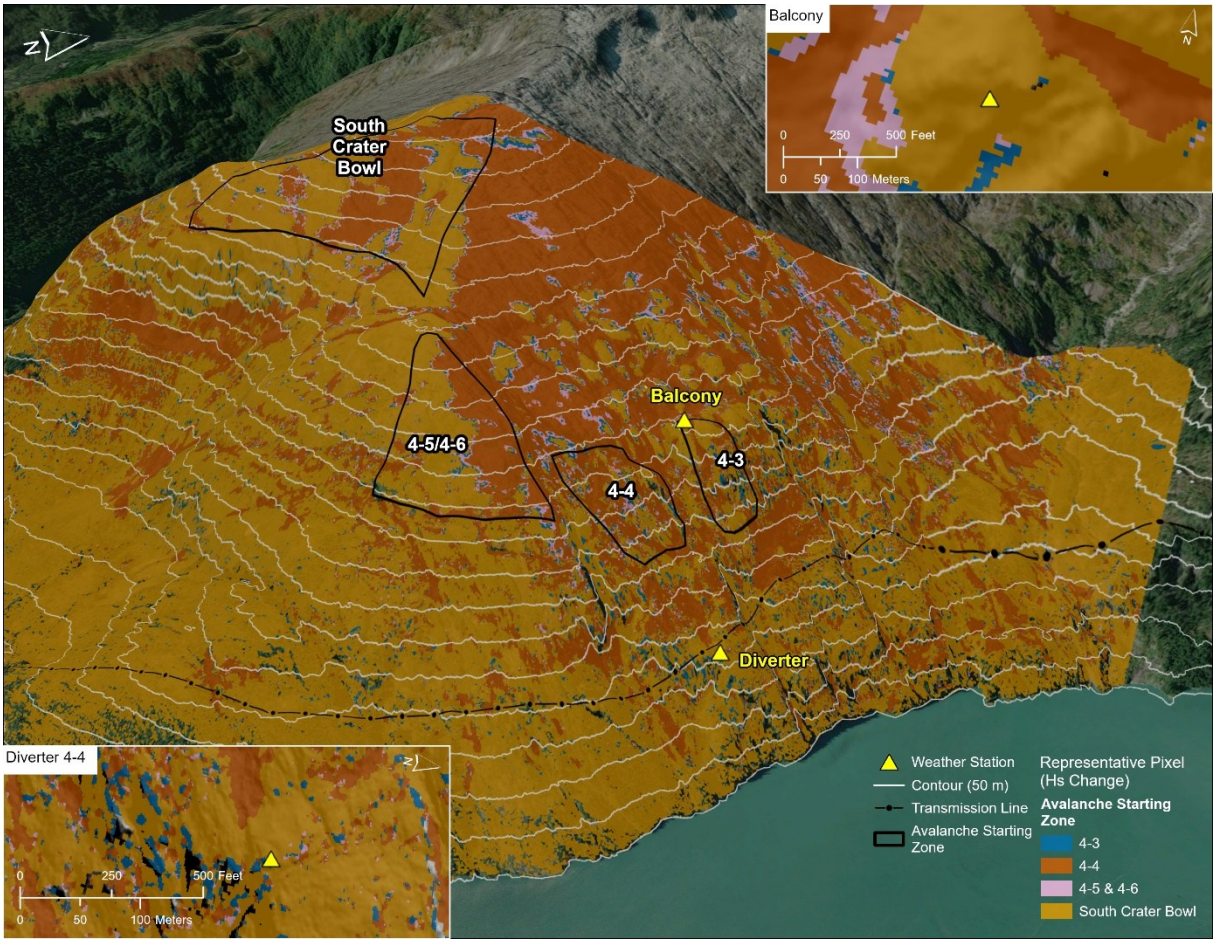


Figure 7: Snow depth *change* representativeness based on Euclidean distance similarity analysis. Raster pixels are colored based on which starting zone they are most similar. Analysis based on change in snow depth during February 2-March 13, 2020, and March 4-April 16, 2021.

REFERENCES

Esri., 2024: How inverse distance weighted interpolation works. ArcGIS Pro Documentation. https://pro.arcgis.com/en/pro-app/latest/help/analysis/geostatistical-analyst/how-inverse-distance-weighted-interpolation-works.htm

Campbell Scientific, 2026: SR50A-Series. Sonic Ranging Sensors. Product Manual. https://s.campbellsci.com/documents/us/manuals/sr50a-series.pdf (downloaded 5/8/2026 at 11:34 am)

Grünewald, T. and Lehning, M., 2011: Altitudinal dependency of snow amounts in two small alpine catchments: can catchment-wide snow amounts be estimated via single snow or precipitation stations?. Annals of Glaciology. 52. 153-158. 10.3189/172756411797252248.

Herbert, J. N., Raleigh, M. S., and Small, E. E., 2024.: Reanalyzing the spatial representativeness of snow depth at automated monitoring stations using airborne lidar data, The Cryosphere, 18, 3495–3512, https://doi.org/10.5194/tc-18-3495-2024, 2024.

McClung, D., and Schaerer, P., 2006: The Avalanche Handbook. 3rd Edition, Mountaineers Books.

Peitzsch, E., Fagre, D., Hendrikx, J., and Birkeland, K., 2018: Detecting snow depth change in avalanche path starting zones using uninhabited aerial systems and structure from motion photogrammetry, Proceedings, International Snow Science Workshop, Innsbruck, Austria, 2018, p. 408-412

Wikstrom Jones, K.M., and Wolken, G.J., 2022: Lidar-derived elevation data for Speel Arm, Southeast Alaska, collected September 7, 2019: Alaska Division of Geological & Geophysical Surveys Raw Data File 2021-11, 8 p. https://doi.org/10.14509/30730